Thermal pairing treatment within the path integral formalism

M. Fellah N.H. Allal[†] M. R. Oudih

Laboratoire de Physique Théorique- Faculté de Physique- USTHB, BP32 El-Alia, 16111 Bab-Ezzouar - Alger - Algeria

Abstract: A method for the treatment of pairing correlations at finite temperature is proposed within the path integral formalism, based on the square root extraction of the pairing term in the Hamiltonian of the system. Gap equations and expressions for the pairing gap parameter Δ, energy E, and heat capacity C are established. The formalism is first tested using the Richardson model, which enables comparison with an exact solution. The results obtained using this formalism are also compared with the finite temperature BCS (FTBCS) results. An improvement over the FTBCS model is noted, especially at low temperatures. Indeed, the agreement between the Δ values of this study and the exact values is good at low temperatures. This leads to better agreement between the values of E and C of this model and the exact values than with the FTBCS values. However, a critical value of temperature remains. Subsequently, realistic cases are considered using single-particle energies of a deformed Woods-Saxon mean-field for the nuclei ^{162}Dy and ^{172}Yb. In the framework of the current approach, pairing effects persist beyond the FTBCS critical temperature. Moreover, at low temperatures, a good agreement between the model and semiexperimental values of the heat capacity is observed, and a clear improvement compared to the FTBCS method is noted. This is no more the case at higher temperatures.

Keywords: nuclear structure, pairing, temperature

DOI: 10.1088/1674-1137/ad641a

I. INTRODUCTION

Pairing correlations are a crucial issue in nuclear structure theory and have been the subject of numerous studies since they were first highlighted at the end of the 1950s [1]. The theory of superfluid states in nuclei was then developed by adapting the Bardeen, Cooper, and Schrieffer (BCS) theory [2] to nuclear physics [3]. However, the typical BCS theory in nuclear physics is a zero-temperature theory. Since the early 1960s, the generalization of the study of nuclear superfluidity at finite temperature has been the subject of considerable attention. This interest has not diminished over the last 60 years, and the subject is still relevant, especially for the study of nuclear processes in hot stellar environments [4−6]. Several studies have been devoted to pairing correlations in heated nuclei. Some used a statistical method based on the BCS theory (see, e.g., Refs. [7−13]) or Hartree-Fock-Bogoliubov (HFB) theory (see, e.g., Refs. [14−18]), before or after particle-number projection. Other studies were based on the temperature dependent random phase approximation (RPA), see, e.g., Refs. [19−22]. For a review, see Ref. [23]. Pairing in hot nuclei has also been investigated in the relativistic case using the relativistic Hartree-Bogoliubov model [24], relativistic finite temperature quasiparticle RPA [6], and covariant density functional theory [25−29].

Recently, the Matsubara formalism [30] and self-consistent Green's function approach [31] have also been used to describe nuclear superfluidity at finite temperature.

Another possible approach for the treatment of pairing correlations in heated systems is based on the path integral representation of the partition function, which involves the shell-model Monte-Carlo method [32−34]. However, this method is not easy to apply, especially for heavy systems with large particle-numbers. Therefore, the static-path approximation (SPA) [35−41] is considered a convenient method of obtaining an approximation of the partition function.

In Ref. [42], Fletcher used the path integral technique, starting with an approximation in the pairing Hamiltonian and then linearizing it using the Hubbard-Stratonovitch transformation [43, 44]. He then showed that the standard finite temperature BCS (FTBCS) gap equations can be obtained via a saddle-point approximation in the path integral representation of the partition function of the system. This method has also been used in the neutron-proton pairing scenario [45−48].

In this study, we propose an alternative method to in-

Received 13 May 2024; Accepted 17 July 2024; Published online 18 July 2024

[†] E-mail: allaln@yahoo.com

vestigate pairing correlations at finite temperature within the path integral formalism. It is based on the polar decomposition of the creation and annihilation operators of pairs of paired particles in the Hamiltonian of a system. The pairing term in the Hamiltonian is then written in square form, which enables direct use of the Hubbard-Stratonovitch transformation.

The paper is organized as follows. Secs. II and III describe the Hamiltonian of the system and the derivation of the partition function, respectively. Expressions for the various statistical quantities are derived in Sec. IV. In Sec. V, the formalism is tested using the Richardson model, which enables comparison with an exact solution. Realistic cases are then considered using single-particle energies of a deformed Woods-Saxon mean-field. Finally, the main conclusions are summarized in Sec. VI.

II. HAMILTONIAN

In the second quantization formalism, the intrinsic motion of a system of paired particles (neutrons or protons) is described by the Hamiltonian

$$\mathcal{H} = \sum_{\nu>0} \varepsilon_\nu (\eta_\nu + \eta_{\tilde{\nu}}) - H_p, \tag{1}$$

where ε_ν is the single-particle energy of the state $|\nu\rangle = a_\nu^+ |0\rangle$ and of its time reverse $|\tilde{\nu}\rangle = a_{\tilde{\nu}}^+ |0\rangle$. η_ν is defined by

$$\eta_\nu = a_\nu^+ a_\nu. \tag{2}$$

The pairing strength G is assumed to be constant, and H_p is defined by

$$H_p = G P^+ P, \tag{3}$$

where

$$P^+ = \sum_{\nu>0} a_\nu^+ a_{\tilde{\nu}}^+. \tag{4}$$

This method is based on the polar decomposition of the operators P^+ and P to obtain the P^+P product on a square form, i.e.,

$$P^+ P = R^2. \tag{5}$$

Therefore, we set $\mathcal{S}_\nu$ the operator

$$\mathcal{S}_\nu = \mathrm{i}\left(a_\nu + a_\nu^+\right)\left(a_{\tilde{\nu}} + a_{\tilde{\nu}}^+\right), \tag{6}$$

where i is the imaginary unit.

$\mathcal{S}_\nu$ obeys the following properties:

$$\mathcal{S}_\nu^+ = \mathcal{S}_\nu \text{ and } \mathcal{S}_\nu^2 = \mathbf{1}. \tag{7}$$

We set

$$U = \prod_{\nu>0} \mathcal{S}_\nu, \tag{8}$$

where U is a unitary operator, which is also given by

$$U = \exp\left[\mathrm{i}\frac{\pi}{2}\sum_{j>0}\left(a_j^+ + a_j + a_{\tilde{j}}^+ + a_{\tilde{j}} - 1\right)\right]. \tag{9}$$

It may then be easily shown that

$$P^+ U = -\mathrm{i}R \quad \text{where } R = \sum_{\nu>0} \eta_\nu \eta_{\tilde{\nu}} B_\nu \tag{10}$$

with

$$B_\nu = \prod_{\substack{j>0 \\ j\neq\nu}} \mathcal{S}_j. \tag{11}$$

In the same manner, we have

$$U^+ P = \mathrm{i}R. \tag{12}$$

This is also the case reciprocally.

Eqs. (10) and (12) represent the generalization, in terms of operators, of the polar decomposition of complex numbers. Indeed,

$$P^+ = R\,\mathrm{e}^{-\mathrm{i}\frac{\pi}{2}}\,U^+ \text{ and } P = \mathrm{e}^{\mathrm{i}\frac{\pi}{2}}\,U\,R. \tag{13}$$

Thus,

$$P^+P = P^+UU^+P = R^2\,. \tag{14}$$

The calculation details of U, P^+P , and R^2 are given in Appendix A.

III. GRAND PARTITION FUNCTION

To conserve the particle number on average, let us define the auxiliary Hamiltonian as

$$H = H_0 - GR^2, \tag{15}$$

where

$$H_0 = \sum_{\nu>0} (\varepsilon_\nu - \lambda)(\eta_\nu + \eta_{\bar{\nu}}), \tag{16}$$

λ being the Fermi energy.

The grand partition function is given by

$$Z = \mathrm{Tr} e^{-\beta H}, \tag{17}$$

where β is the inverse of the temperature T of the system, and Tr is the trace over all the states of the system.

Note that H_0 and H_p do not commute, thus

$$e^{-\beta H} \neq e^{-\beta H_0} e^{\beta H_p}. \tag{18}$$

We now consider the operator $\mathsf{S}(\beta)$ defined as

$$e^{-\beta H} = e^{-\beta H_0} \mathsf{S}(\beta), \tag{19}$$

that is,

$$\mathsf{S}(\beta) = e^{\beta H_0} e^{-\beta H}. \tag{20}$$

We can easily show that $\mathsf{S}(\beta)$ satisfies the differential equation

$$\frac{\partial \mathsf{S}(\beta)}{\partial \beta} = e^{-\beta H_0} H_p e^{-\beta H} = H_p(\beta) \mathsf{S}(\beta), \tag{21}$$

where $H_p(\beta)$ is the Heisenberg transform of H_p

$$H_p(\beta) = e^{\beta H_0} H_p e^{-\beta H_0}. \tag{22}$$

Eq. (21) is easily solved, considering the initial condition $\mathsf{S}(\beta = 0) = \mathbf{1}$. The implicit solution is then

$$\mathsf{S}(\beta) = \mathbf{1} + \int_0^\beta H_p(\tau_1) \mathsf{S}(\tau_1) \mathrm{d}\tau_1 \quad , \ 0 \leqslant \tau_1 \leqslant \beta. \tag{23}$$

By proceeding by iteration, $\mathsf{S}(\beta)$ may be formally written as

$$\mathsf{S}(\beta) = T_\tau \exp\left(\int_0^\beta H_p(\tau) \mathrm{d}\tau \right) \tag{24}$$

T_τ is the chronological operator.

Then, Z may be expressed as

$$Z = \mathrm{Tr} e^{-\beta H_0} \mathsf{S}(\beta) \tag{25}$$

where

$$\mathsf{S}(\beta) = T_\tau \exp\left(\int_0^\beta G R^2(\tau) \mathrm{d}\tau \right), \tag{26}$$

$R(\tau)$ being the Heisenberg transform for the imaginary time τ of the operator R:

$$R(\tau) = e^{-\tau H_0} R e^{\tau H_0}. \tag{27}$$

In the integral in Eq. (26), the interval $[0,\beta]$ is divided into N intervals of length $\frac{\beta}{N}$. Therefore, by definition,

$$G \int_0^\beta R^2(\tau) \mathrm{d}\tau = \lim_{N\to\infty} \exp\left[\frac{\beta G}{N} \sum_{j=1}^N R^2(\tau_j) \right]; \tau_j = j\frac{\beta}{N}, \tag{28}$$

because

$$\begin{aligned} \int_0^\beta f(X(\tau)) \mathrm{d}\tau &= \lim_{N\to\infty} \frac{\beta}{N} \sum_{j=1}^N f\left(X(\tau_j)\right) \\ &= \lim_{N\to\infty} \frac{\beta}{N} \sum_{j=1}^N f\left(X_j\right), \end{aligned} \tag{29}$$

where $f(x)$ is any integrable function on the interval $[0,\beta]$.

Thus,

$$\mathsf{S}(\beta) = \lim_{N\to\infty} T_\tau \prod_{j=1}^N \exp\left[\frac{\beta G}{N} R^2(\tau_j) \right]. \tag{30}$$

Using the Hubbard-Stratonovitch transformation [42−44],

$$\exp\left(O^2\right) = \int_{-\infty}^{+\infty} \mathrm{d}x \exp\left\{ -\pi x^2 - 2\sqrt{\pi} x O \right\}, \tag{31}$$

where O is a bounded Hermitian operator, and x is an external field, $\mathsf{S}(\beta)$ may be written as

$$\begin{aligned} \mathsf{S}(\beta) = \lim_{N\to\infty} T_\tau \prod_{j=1}^N \int_{-\infty}^{+\infty} \mathrm{d}x_j \\ \times \exp\left\{ -\pi x_j^2 - 2x_j \sqrt{\frac{\pi\beta G}{N}} R(\tau_j) \right\}, \end{aligned} \tag{32}$$

where we set

$$x_j = x(\tau_j)$$

to simplify the notations.

Let us set

$$x_j = \sqrt{\frac{\beta}{N}}X_j \text{ and } \int \mathfrak{D}X = \lim_{N\to\infty}\int_{-\infty}^{+\infty}\prod_{j=1}^{N}\sqrt{\frac{\beta}{N}}\mathrm{d}X_j. \quad (33)$$

It is worth noting that X_j refers to $X(\tau_j)$ and when the limit is taken, $X_j \to X(\tau)$.

We then have

$$\mathsf{S}(\beta) = T_\tau \int \mathfrak{D}X \times \exp\left\{-\pi\int_0^\beta X^2(\tau)d\tau - 2\sqrt{\pi G}\int_0^\beta X(\tau)R(\tau)\mathrm{d}\tau\right\}. \quad (34)$$

We set

$$\Delta(\tau) = \sqrt{\pi G}X(\tau). \quad (35)$$

Using the SPA [49], where it is assumed that $\Delta(\tau)$ is independent of τ, i.e.,

$$\Delta(\tau) = \Delta, \quad (36)$$

Z reduces to an ordinary integral over the variable Δ. It then reads as

$$Z = \mathrm{Tr}\frac{1}{\sqrt{\pi G}}\int \mathrm{d}\Delta \exp\left\{-\frac{\beta}{G}|\Delta|^2 - \beta\left[H_0 + 2\Delta\sum_\nu \eta_\nu\eta_{\tilde{\nu}}B_\nu\right]\right\}. \quad (37)$$

After some algebra, it is given by

$$Z = \frac{1}{\sqrt{\pi G}}\mathrm{Tr}\int \mathrm{d}\Delta \exp\left[-\frac{\beta}{G}|\Delta|^2 - \beta\sum_\nu h_\nu\right], \quad (38)$$

where we set

$$h_\nu = \tilde{\varepsilon}_\nu(\eta_\nu + \eta_{\tilde{\nu}}) + 2\Delta\eta_\nu\eta_{\tilde{\nu}}B_\nu \text{ and } \tilde{\varepsilon}_\nu = \varepsilon_\nu - \lambda. \quad (39)$$

The eigenvalues of η_ν are 0 and 1, which acts on a two-dimensional space. In its eigenbasis, its matrix (η_ν) is

$$(\eta_\nu) = \begin{pmatrix} 0 & 0 \\ 0 & 1 \end{pmatrix}. \quad (40)$$

In the same manner, the eigenvalues of $\eta_{\tilde{\nu}}$ are 0 and 1 and its matrix $(\eta_{\tilde{\nu}})$, in its eigenbasis, is given by

$$(\eta_{\tilde{\nu}}) = \begin{pmatrix} 0 & 0 \\ 0 & 1 \end{pmatrix}. \quad (41)$$

As for B_ν, knowing that $B_\nu^2 = \mathbf{1}$, its eigenvalues are (-1) and 1. Its matrix (B_ν) is given, in its eigenbasis, by

$$(B_\nu) = \begin{pmatrix} -1 & 0 \\ 0 & 1 \end{pmatrix}. \quad (42)$$

The eigenbasis of h_ν is the tensor product of the eigenbases of the three operators. The eigenvalues of η_ν, $\eta_{\tilde{\nu}}$, and B_ν in this space are given in Table 1.

However, these three operators commute with each other and act on different spaces. Knowing the eigenvalues of η_ν, $\eta_{\tilde{\nu}}$, and B_ν, the eigenvalues of h_ν can be deduced for a given ν using Table 1. Thus,

$$\mathrm{Tr}\,\mathrm{e}^{-\beta h_\nu} = 2\left[1 + 2\mathrm{e}^{-\beta\tilde{\varepsilon}_\nu} + \mathrm{e}^{-2\beta\tilde{\varepsilon}_\nu}\cosh(2\beta\Delta)\right]. \quad (43)$$

Next, to calculate the trace in Eq. (38), we assume, as an approximation, that h_ν and h_μ commute when $\nu \neq \mu$. Indeed, the commutator $[h_\nu, h_\mu]$ is given by

$$\begin{aligned}[h_\nu, h_\mu] = {} & 2\Delta\left\{\tilde{\varepsilon}_\nu\left[\eta_\nu + \eta_{\tilde{\nu}}, \eta_\mu\eta_{\tilde{\mu}}B_\mu\right]\right. \\ & \left. + \tilde{\varepsilon}_\mu\left[\eta_\nu\eta_{\tilde{\nu}}B_\nu, \eta_\mu + \eta_{\tilde{\mu}}\right]\right\} \\ & + 4\Delta^2\left[\eta_\nu\eta_{\tilde{\nu}}B_\nu, \eta_\mu\eta_{\tilde{\mu}}B_\mu\right]. \end{aligned} \quad (44)$$

It is thus the sum of a term proportional to G and a term proportional to $\sqrt{G}$, because $\Delta = X\sqrt{\pi G}$. The value of G is generally small compared to single-particle energies, justifying the approximation. This results in

$$\mathrm{Tr}\exp\left(-\beta\sum_\nu h_\nu\right) = \prod_\nu \mathrm{Tr}\,\mathrm{e}^{-\beta h_\nu}. \quad (45)$$

As a consequence, the partition function may be written as

Table 1. Eigenvalues of η_ν, $\eta_{\tilde{\nu}}$, B_ν, and h_ν.

η_ν	0	0	0	0	1	1	1	1
$\eta_{\tilde{\nu}}$	0	0	1	1	0	0	1	1
B_ν	−1	1	−1	1	−1	1	−1	1
h_ν	0	0	$\tilde{\varepsilon}_\nu$	$\tilde{\varepsilon}_\nu$	$\tilde{\varepsilon}_\nu$	$\tilde{\varepsilon}_\nu$	$2\tilde{\varepsilon}_\nu - 2\Delta$	$\tilde{\varepsilon}_\nu + 2\Delta$

$$Z = \frac{1}{\sqrt{\pi G}} \int \mathrm{d}\Delta \mathrm{e}^{-\frac{\beta}{G}|\Delta|^2} \times \prod_{\nu} \left\{ \quad 2\left[1 + 2\mathrm{e}^{-\beta\tilde{\varepsilon}_\nu} + \mathrm{e}^{-2\beta\tilde{\varepsilon}_\nu} \cosh(2\beta\Delta)\right] \right\}. \tag{46}$$

It is worth noting that this approach differs from the Fletcher method [42], which is recalled in Appendix B. In the latter, the pairing term in Eq. (B3) is written as a product $\theta_1\theta_2$ and then converted into a square form to apply the Hubbard-Stratonovitch transformation. In the present study, the pairing term is in square form, enabling direct application of the Hubbard-Stratonovitch transformation.

However, in both approaches, an approximation is made because θ_1 and θ_2 are assumed to commute in the Fletcher method and h_ν and h_μ, $\nu \neq \mu$, are assumed to commute in this study.

At this stage, it is difficult to determine whether the approximations are justified. However, a comparison of the numerical results of the various statistical quantities with exact values obtained within a schematic model will enable us to judge the validity of the approximations (see Sec. V).

IV. STATISTICAL QUANTITIES

The grand partition function can be used to determine various statistical quantities, such as energy, entropy, and heat capacity.

A. Free energy

The free energy is obtained using the relation

$$Z = \frac{1}{\sqrt{\pi G}} \int \mathrm{d}\Delta \mathrm{e}^{-\beta F} \tag{47}$$

and thus,

$$F = \frac{\Delta^2}{G} - \frac{1}{\beta} \sum_{\nu} \ln\left\{2\left[1 + 2\mathrm{e}^{-\beta\tilde{\varepsilon}_\nu} + \mathrm{e}^{-2\beta\tilde{\varepsilon}_\nu} \cosh(2\beta\Delta)\right]\right\}. \tag{48}$$

B. Gap parameter

The quantity Δ is interpreted as the gap parameter. Hereafter, it is assumed to be real. It is found using the saddle point approximation [50]

$$\frac{\partial F}{\partial \Delta} = 0. \tag{49}$$

Indeed, the dominant contribution to the partition function is found by determining the minimum value of the exponent in Eq. (47), resulting in

$$\frac{\Delta}{G} = \sinh(2\beta\Delta) \sum_{\nu} \frac{\mathrm{e}^{-2\beta\tilde{\varepsilon}_\nu}}{1 + 2\mathrm{e}^{-\beta\tilde{\varepsilon}_\nu} + \mathrm{e}^{-2\beta\tilde{\varepsilon}_\nu}.\cosh(2\beta\Delta)} = \sinh(2\beta\Delta) \sum_{\nu} \frac{1}{D_\nu}, \tag{50}$$

where

$$D_\nu = \left(1 + \mathrm{e}^{\beta\tilde{\varepsilon}_\nu}\right)^2 + 2\sinh^2(\beta\Delta). \tag{51}$$

C. Particle-number

Because the grand potential Ω is given by

$$\Omega = -\beta F, \tag{52}$$

and the particle-number is defined by

$$N = \left.\frac{\partial \Omega}{\partial \alpha}\right|_{\beta=\text{const.}}, \quad \alpha = \beta\lambda, \tag{53}$$

we obtain

$$N = 2\sum_{\nu} N_\nu, \tag{54}$$

with

$$N_\nu = 1 - \frac{\mathrm{e}^{\beta\tilde{\varepsilon}_\nu} + \mathrm{e}^{2\beta\tilde{\varepsilon}_\nu}}{D_\nu}. \tag{55}$$

The system of Eqs. (50) and (54) constitutes the gap equations.

The quantity N_ν may also be written as

$$N_\nu = \frac{\mathrm{e}^{-\beta\tilde{\varepsilon}_\nu} + \mathrm{e}^{-2\beta\tilde{\varepsilon}_\nu}.\cosh(2\beta\Delta)}{1 + 2\mathrm{e}^{-\beta\tilde{\varepsilon}_\nu} + \mathrm{e}^{-2\beta\tilde{\varepsilon}_\nu}.\cosh(2\beta\Delta)}. \tag{56}$$

D. Energy of the system

The energy of the system is defined as

$$E = -\left.\frac{\partial \Omega}{\partial \beta}\right|_{\alpha=\text{const.}}. \tag{57}$$

Then, after some algebra,

$$E = -\frac{\Delta^2}{G} + 2\sum_{\nu} \varepsilon_\nu N_\nu. \tag{58}$$

E. Entropy

The entropy is defined by

$$S = \Omega - \beta\lambda N + \beta E. \tag{59}$$

After all calculations, it reads as

$$S = -2\beta\frac{\Delta^2}{G} + 2\beta\sum_{\nu}\tilde{\varepsilon}_{\nu}N_{\nu} + \sum_{\nu}\ln 2\left[1 + 2\mathrm{e}^{-\beta\tilde{\varepsilon}_{\nu}} + \mathrm{e}^{-2\beta\tilde{\varepsilon}_{\nu}}.\cosh(2\beta\Delta)\right]. \tag{60}$$

F. Heat capacity

The heat capacity of the system is defined by

$$C = -\beta\frac{\partial S}{\partial\beta}. \tag{61}$$

After some algebra, $\frac{\partial S}{\partial\beta}$ may be written as

$$\frac{\partial S}{\partial\beta} = \frac{2\Delta^2}{G} - \frac{2\Delta}{G}\frac{\partial(\beta\Delta)}{\partial\beta} + 2\beta\sum_{\nu}\tilde{\varepsilon}_{\nu}\frac{\partial N_{\nu}}{\partial\beta}, \tag{62}$$

where

$$\frac{\partial N_{\nu}}{\partial\beta} = -\frac{\tilde{\varepsilon}_{\nu}\mathrm{e}^{2\beta\tilde{\varepsilon}_{\nu}}}{D_{\nu}} + (1-N_{\nu})\left[\tilde{\varepsilon}_{\nu}(1-2N_{\nu}) + 2\sinh(2\beta\Delta)\frac{\partial(\beta\Delta)}{\partial\beta}\frac{1}{D_{\nu}}\right], \tag{63}$$

and $\frac{\partial(\beta\Delta)}{\partial\beta}$ is deduced from the relation

$$\frac{\partial(\beta\Delta)}{\partial\beta}\left[\frac{1}{G} - 2\beta\frac{\Delta}{G}\coth(2\beta\Delta)\sum_{\nu}\frac{1}{D_{\nu}} + 2\beta\sinh^2(2\beta\Delta)\sum_{\nu}\frac{1}{D_{\nu}^2}\right] = \frac{\Delta}{G} - 2\beta\sinh(2\beta\Delta)\sum_{\nu}\frac{\tilde{\varepsilon}_{\nu}(1-N_{\nu})}{D_{\nu}}. \tag{64}$$

Note that the obtained expressions for the various statistical quantities are different from those of the FTBCS approach, which are recalled in Appendix B.

V. NUMERICAL RESULTS AND DISCUSSION

The previously described formalism is first applied to the Richardson model, enabling comparison with an exact solution. Subsequently, it is applied to realistic cases.

A. Richardson model

In this section, we use the Richardson model with the same parameters as in Ref. [51], which refers to the exact solution of Ref. [52]. Thus, we consider $N = 10$, $G = 0.4$ and doubly degenerated equidistant levels such that

$$\varepsilon_i = \left(i - \frac{1}{2}(N_{or}+1)\right)\Delta\varepsilon\,, \quad i = 1,2,...,N_{or}, \tag{65}$$

N_{or} is the total degeneracy of the levels, with $N_{or} = 10$ and $\Delta\varepsilon = 1$.

The various statistical quantities are then calculated as functions of temperature T using the approach in this study and compared with the exact solution and FTBCS results. The variations in the pairing gap parameter Δ, energy E, and heat capacity C are shown in Fig. 1.

As shown in the figure, the overall behavior of $\Delta(T)$ is similar to the typical behavior in the FTBCS approach, i.e., exhibiting a plateau on a given interval at low temperatures and then decreasing until Δ vanishes at the critical temperature T_c. The sharp phase transition at $T = T_c$ is due to the approximations used in this study, i.e., the

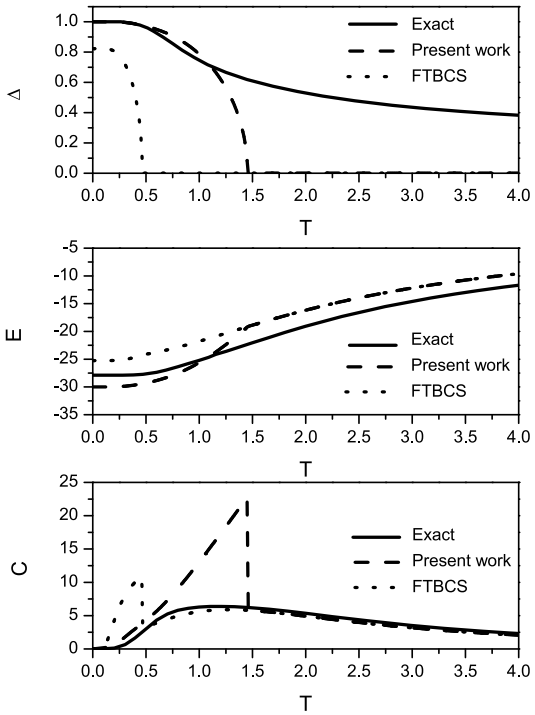

Fig. 1. Variations in the pairing gap parameter Δ (upper part), energy E (middle), and heat capacity C (lower part) as functions of temperature T. The solid lines refer to the exact results, and the dashed and dotted lines refer to the results of this study and FTBCS, respectively.

SPA (Eq. (36)), that of Eq. (45), and the saddle-point approximation (Eq. (49)). The inclusion of quantal and thermal fluctuations may lead to smoother behavior.

Furthermore, the agreement between the values of Δ from this study and the exact values is good for $0 \leqslant T \leqslant 0.5$; a clear improvement in the Δ values of this study compared to the FTBCS values should be noted. Indeed, the FTBCS method predicts a Δ value of approximately 0.8 at low temperatures, whereas the present model reproduces the exact value $\Delta = 1$.

Moreover, the T_c value of this study is clearly larger than that of the FTBCS approach. Consequently, our model better reproduces the exact values of Δ over a larger temperature interval. Indeed, our values are relatively close to the exact values until $T \simeq 1.2$.

The behavior of $E(T)$ at low temperatures is similar in the three cases. However, our model leads to a decrease in energy with respect to the exact values of approximately 7%, whereas the FTBCS method leads to an increase of approximately 9%. At higher temperatures, the difference in the Δ shape leads to a difference in the shape of the energy.

Finally, as shown in Fig. 1, the shape of the heat capacity C at low temperatures, i.e., at $0 \leqslant T \leqslant 0.5$, is closer to that of the exact solution than that of the FTBCS method. Of course, the discontinuity at $T = T_c$ still exists.

For large values of T, i.e., beyond the critical temperature of the FTBCS method and this study, the pairing vanishes. Thus, the energy is the same in both models. However, it may seem surprising that in this region, the C values of both models reproduce the exact values, whereas the exact value of Δ does not vanish. This is because the $E(T)$ curves (and thus those of $S(T)$) are parallel in this region; therefore, the value of the derivative is the same.

B. Realistic cases

Next, we choose two nuclei as illustrative examples : ^{162}Dy and ^{172}Yb. These nuclei have semiexperimental heat capacity data, allowing comparisons with the current results. The single-particle energies are those of a Woods-Saxon deformed mean-field using the parameters described in Ref. [53], with a maximum number of shells $N_{\max} = 12$.

To enable comparisons with the FTBCS approach, the pairing strength G is chosen to reproduce the pairing gap parameters Δ at zero temperature in both approaches, which are deduced from the even-odd mass differences and given by [54]

$$\Delta_p = -\frac{1}{8}[M(Z+2,N) - 4M(Z+1,N) + 6M(Z,N) - 4M(Z-1,N) + M(Z-2,N)], \quad (66)$$

$$\Delta_n = -\frac{1}{8}[M(Z,N+2) - 4M(Z,N+1) + 6M(Z,N) - 4M(Z,N-1) + M(Z,N-2)], \quad (67)$$

for the proton and neutron systems, respectively. $M(Z,N)$ is the experimental mass value.

For the same reason, we consider the excitation energy $E_{\rm exc}$ defined as

$$E_{\rm exc} = E(T) - E(0), \quad (68)$$

rather than the energy of the system.

The variations in the gap parameter Δ, excitation energy $E_{\rm exc}$, and heat capacity C as functions of temperature T are shown in Figs. 2 and 3 for the proton and neutron systems of the two nuclei mentioned above. The FTBCS results are shown in the same figures.

In each case, the overall behavior of $\Delta(T)$ is similar to the typical behavior in the FTBCS approach, as is the case in the schematic example. Once again, the T_c values

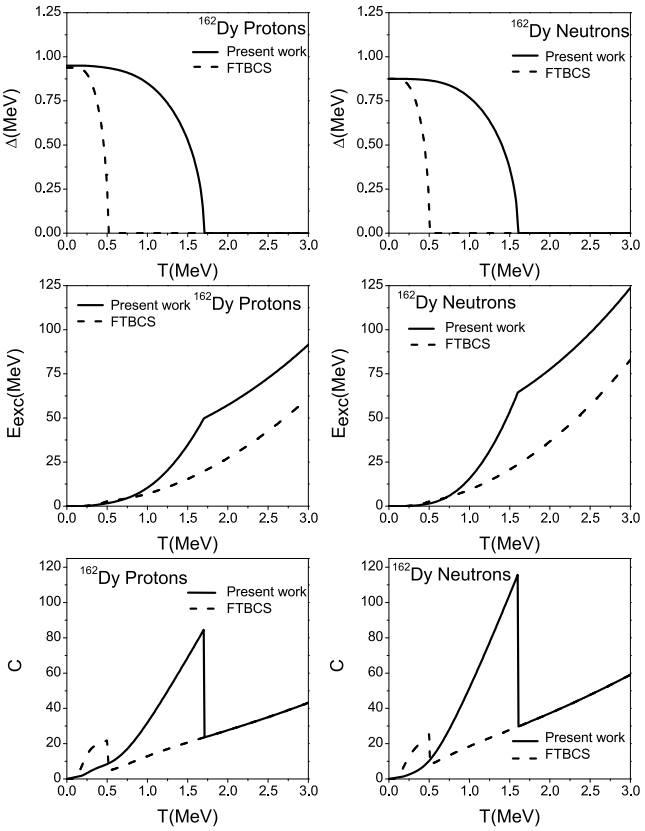

Fig. 2. Variations in the pairing gap parameter Δ (upper part), excitation energy $E_{\rm exc}$ (middle), and heat capacity C (lower part) as functions of temperature T for the proton (left) and neutron (right) systems of ^{162}Dy. The solid lines refer to the results of this study, and the dashed lines are the FTBCS results.

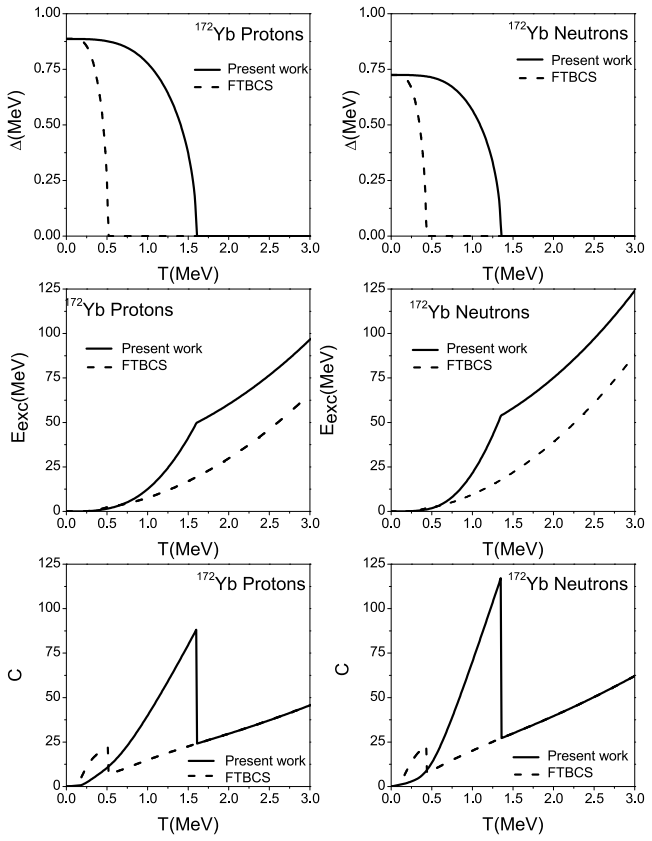

Fig. 3. Same as Fig. 2, but for ^{172}Yb.

of this study are clearly more important than those of the FTBCS approach. The ratio $T_c/(T_c)_{\rm FTBCS}$ is close to 3.

The behavior of the pairing parameters is reflected in the excitation energy, and the curves are similar in both approaches. We note a change in the slope at $T = T_c$. In the region $T < (T_c)_{\rm FTBCS}$, $E_{\rm exc}$ increases more rapidly in the FTBCS approach than in this study. In the region $(T_c)_{\rm FTBCS} < T < T_c$, $E_{\rm exc}$ in this study increases significantly faster than in the FTBCS case. In fact, in this region, the FTBCS pairing gap is nil. No explanation for this behavior is found, nor for $E_{\rm exc}$ being larger in the present model. Finally, when $T > T_c$, the curves of the two approaches are parallel.

Regarding the heat capacity, we can draw the same conclusions regarding the general features of the curves deduced from the two approaches. The sharp discontinuity in C observed at $T = T_c$ within the conventional FTBCS approach remains when using our formalism. However, it is worth noting that the graphs join beyond T_c, when the pairing effects vanish.

Next, the total heat capacity C_T is evaluated as a function of temperature for both nuclei, making it possible to compare it with semiexperimental values. The latter are taken from Ref. [13], which refers to Refs. [55] and [56]. The corresponding results are shown in Figs. 4 and 5 for ^{162}Dy and ^{172}Yb, respectively. In both figures, the section within the interval $0 \leqslant T \leqslant 1$ MeV, in which semiexperimental data are available, is enlarged in part (b) for clarity.

In each case (see Figs. 4 (a) and 5 (a)), two discontinuities are noted, corresponding to the neutron and proton critical temperatures, within the current model and FTBCS approach. In the ^{162}Dy case, the two FTBCS critical temperatures are very close to each other, revealing only a discontinuity in the curve.

Note that the FTBCS curves of this study show, in each case, a sharp increase at low temperatures, whereas in Refs. [57] (for ^{162}Dy) and [13] (for both ^{162}Dy and ^{172}Yb), C is flat in this region. This difference is likely due to the choice of the pairing-strength G value. In this study, we do not use the same value of G for the two approaches (i.e., the FTBCS and present approaches). As highlighted above, the G values are chosen to reproduce the Δ value at zero temperature in each case.

Moreover, for both nuclei, beyond the proton system

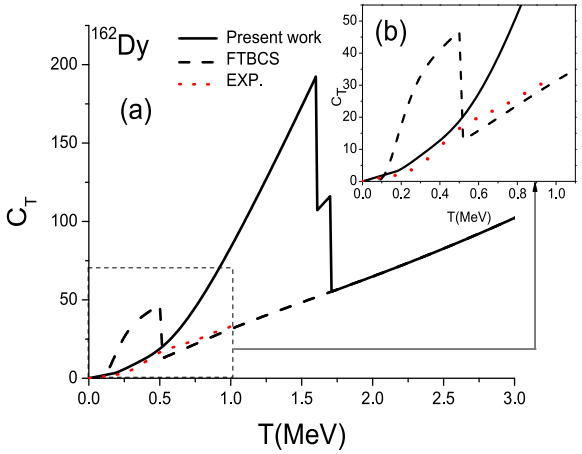

Fig. 4. (color online) Variation in the total heat capacity of ^{162}Dy as a function of temperature T. The solid lines refer to the results of this study, the dashed lines are the FTBCS results, and the dotted lines are the values extracted from experimental data.

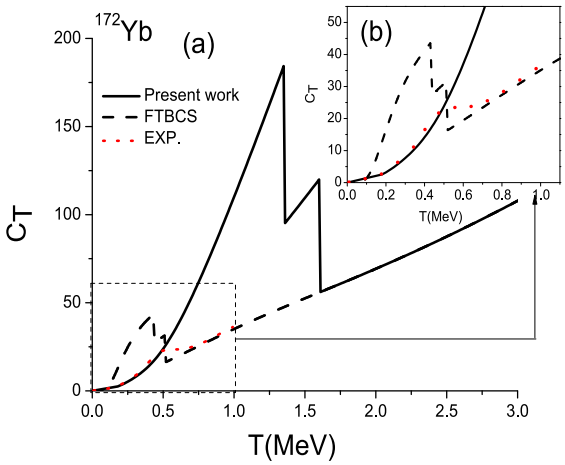

Fig. 5. (color online) Same as Fig. 4, but for ^{172}Yb.

critical temperature of the present model, the curves of the two models are superposed because there is no more pairing in this region.

As clearly shown in Figs. 4 (b) and 5 (b), at low temperatures, i.e., when $T \leqslant 0.5$ MeV, the agreement between the results of this study and the semiexperimental values is good, which is not the case for the FTBCS method. This observation is consistent with the conclusions drawn in the case of the Richardson model.

In addition, as in the schematic case, the good agreement between the values obtained using our model and the experimental (respectively exact) values is observed in the interval where Δ has a plateau shape.

Paradoxically, the FTBCS method seems to better reproduce the experimental values in the interval between the proton system critical temperatures of the two models. However, note that in this region, the FTBCS method predicts that the pairing effects vanish, suggesting that the entropy curves are parallel in this region, as is the case within the Richardson model.

However, in the present approach, the S shape of the experimental heat capacities is not reproduced. The model predicts a sharp transition when the temperature reaches its critical value. This shortcoming may be overcome by performing particle-number projection before variation (see, e.g., Refs. [13, 41, 57],). In our approach, thermal and quantal fluctuations should also be considered. One should then go beyond the SPA defined by Eq. (36).

VI. CONCLUSION

We present a model for the treatment of nuclear pairing at finite temperature within the path integral formalism, based on the polar decomposition of the creation and annihilation operators of pairs of paired particles in the Hamiltonian of the system. The pairing term in the Hamiltonian is then written in square form, which enables direct use of the Hubbard-Stratonovitch transformation. This facilitates the derivation of the partition function of the system using the SPA.

A new expression for the partition function is established. Gap equations and expressions for various statistical quantities are then derived, which differ from those of the FTBCS approach because the used approximations are not of the same nature.

The model is first numerically tested using the Richardson schematic model, which enables a comparison with the exact solution. The results obtained using the present formalism are also compared to the FTBCS results. An improvement compared to the FTBCS model is noted at low temperatures for the values of the pairing gap parameter Δ. Indeed, our model can be used to reproduce the exact value of Δ, which is not the case of the FTBCS model. An improvement is also noted for the energy E and heat capacity C. However, there is still a critical temperature T_c , which leads to discontinuities in the Δ, E , and C curves. The T_c value of this study is found to be larger than that of FTBCS.

The model is then applied to realistic cases using the single-particle energies of a deformed Woods-Saxon mean-field. The various statistical quantities are evaluated for the proton and neutron systems of the ^{162}Dy and ^{172}Yb nuclei, which are chosen as illustrative examples. Compared to the FTBCS results, the overall behavior of the gap parameters and the various statistical quantities as functions of temperature is similar.

However, in the framework of our approach, the pairing effects persist at temperatures higher than those predicted by the FTBCS approach.

Because semiexperimental data of the heat capacity are available for these two nuclei, we compare them with the predictions of the present model and the FTBCS results. The model in our study better reproduces the experimental values at low temperatures. However, in the interval between the proton system critical temperatures of the two models, the FTBCS method appears to better reproduce the experimental values. This is paradoxical because FTBCS predicts that the pairing effects vanish in this region.

It would be interesting to consider the thermal and quantal fluctuations in the present model and perform particle-number projection. It would also be interesting to extend our formalism to the neutron-proton pairing case.

APPENDIX A: CALCULATION DETAILS OF U, P^+P , AND R^2

Recall that

$$U = \prod_{j>0} \mathcal{S}_j \,, \tag{A1}$$

where

$$\mathcal{S}_j = i\left(a_j + a_j^+\right)\left(a_{\bar{j}} + a_{\bar{j}}\right). \tag{A2}$$

A. Calculation of U

Let us establish Eq. (9). Using Eq. (A2), we have

$$i\mathcal{S}_j = i\left(a_j + a_j^+\right).i\left(a_{\bar{j}} + a_{\bar{j}}^+\right). \tag{A3}$$

First, we establish that

$$i\left(a_j + a_j^+\right) = \exp\left[i\frac{\pi}{2}\left(a_j + a_j^+\right)\right]. \tag{A4}$$

Indeed,

$$\exp\left[\frac{i\pi}{2}\left(a_j+a_j^+\right)\right]=\sum_{n\geqslant 0}\frac{i^{2n}}{(2n)!}\left(\frac{\pi}{2}\right)^{2n}\left(a_j+a_j^+\right)^{2n}+\sum_{n\geqslant 0}\frac{i^{2n+1}}{(2n+1)!}\left(\frac{\pi}{2}\right)^{2n+1}\left(a_j+a_j^+\right)^{2n+1}. \tag{A5}$$

However,

$$\left(a_j+a_j^+\right)^{2n}=\mathbf{1}\ \text{and}\ \ \left(a_j+a_j^+\right)^{2n+1}=a_j^++a_j, \tag{A6}$$

thus,

$$\begin{aligned}\exp\left[\frac{i\pi}{2}\left(a_j+a_j^+\right)\right]&=\sum_{n\geqslant 0}\frac{(-1)^n}{(2n)!}\left(\frac{\pi}{2}\right)^{2n}+i\left(a_j+a_j^+\right)\sum_{n\geqslant 0}\frac{(-1)^n}{(2n+1)!}\left(\frac{\pi}{2}\right)^{2n+1}\\&=\cos\frac{\pi}{2}+i\left(a_j+a_j^+\right)\sin\frac{\pi}{2}\\&=i\left(a_j+a_j^+\right).\end{aligned} \tag{A7}$$

Similarly,

$$i\left(a_{\bar{j}}+a_{\bar{j}}^+\right)=\exp\left[i\frac{\pi}{2}\left(a_{\bar{j}}+a_{\bar{j}}^+\right)\right]. \tag{A8}$$

We then obtain

$$\begin{aligned}i\mathcal{S}_j&=\exp\left[i\frac{\pi}{2}\left(a_j+a_j^+\right)\right]\exp\left[i\frac{\pi}{2}\left(a_{\bar{j}}+a_{\bar{j}}^+\right)\right]\\&=\exp\left[i\frac{\pi}{2}\left(a_j+a_j^++a_{\bar{j}}+a_{\bar{j}}^+\right)\right],\end{aligned} \tag{A9}$$

because a_j and a_j^+ commute with $a_{\bar{j}}$ and $a_{\bar{j}}^+$.

That is,

$$\begin{aligned}\mathcal{S}_j&=-i\exp\left[i\frac{\pi}{2}\left(a_j+a_j^++a_{\bar{j}}+a_{\bar{j}}^+\right)\right]\\&=\exp\left[i\frac{\pi}{2}\left(a_j+a_j^++a_{\bar{j}}+a_{\bar{j}}^+-1\right)\right].\end{aligned} \tag{A10}$$

Using Eq. (A1), we obtain

$$U=\exp\left[i\frac{\pi}{2}\sum_{j>0}\left(a_j+a_j^++a_{\bar{j}}+a_{\bar{j}}^+-1\right)\right]. \tag{A11}$$

B. Equation $P^+P=R^2$

Let us calculate $a_\nu^+a_{\bar{\nu}}^+U$. We have

$$\begin{aligned}a_\nu^+a_{\bar{\nu}}^+U&=a_\nu^+a_{\bar{\nu}}^+\prod_{j>0}\mathcal{S}_j\\&=a_\nu^+a_{\bar{\nu}}^+\mathcal{S}_\nu\prod_{\substack{j>0\\j\neq\nu}}\mathcal{S}_j\\&=-i\eta_\nu\eta_{\bar{\nu}}\prod_{\substack{j>0\\j\neq\nu}}\mathcal{S}_j=-i\eta_\nu\eta_{\bar{\nu}}B_\nu,\end{aligned} \tag{A12}$$

where we set

$$B_\nu=\prod_{\substack{j>0\\j\neq\nu}}\mathcal{S}_j. \tag{A13}$$

Similarly,

$$U^+a_{\bar{\mu}}a_\mu=i\eta_\mu\eta_{\bar{\mu}}\prod_{\substack{j>0\\j\neq\mu}}\mathcal{S}_j=i\eta_\mu\eta_{\bar{\mu}}B_\mu. \tag{A14}$$

using the definition (4) of P^+ and P, i.e.,

$$P^+=\sum_{\nu>0}a_\nu^+a_{\bar{\nu}}^+\ ,\ \ P=\sum_{\mu>0}a_{\bar{\mu}}a_\mu, \tag{A15}$$

we then have

$$P^+U=\sum_{\nu>0}a_\nu^+a_{\bar{\nu}}^+U=-i\sum_{\nu>0}\eta_\nu\eta_{\bar{\nu}}B_\nu=-iR \tag{A16}$$

and

$$U^+P=\sum_{\mu>0}U^+a_{\bar{\mu}}a_\mu=i\sum_{\mu>0}\eta_\mu\eta_{\bar{\mu}}B_\mu=iR \tag{A17}$$

where we set

$$R=\sum_{\nu>0}\eta_\nu\eta_{\bar{\nu}}B_\nu. \tag{A18}$$

Hence,

$$P^+P=P^+UU^+P=R^2. \tag{A19}$$

C. Equation $R^2=P^+P$

We have

$$
\begin{aligned}
R^2 = P^+P &= \left(\sum_{\nu>0}\eta_\nu\eta_{\tilde{\nu}}B_\nu\right)\left(\sum_{\mu>0}\eta_\mu\eta_{\tilde{\mu}}B_\mu\right)\\
&= \left(\sum_{\nu>0}\eta_\nu\eta_{\tilde{\nu}}\prod_{\substack{j>0\\ j\neq\nu}}\mathcal{S}_j\right)\left(\sum_{\mu>0}\eta_\mu\eta_{\tilde{\mu}}\prod_{\substack{j>0\\ j\neq\mu}}\mathcal{S}_j\right)\\
&= \sum_{\nu,\mu>0}\eta_\nu\eta_{\tilde{\nu}}S_\mu\eta_\mu\eta_{\tilde{\mu}}S_\nu\prod_{\substack{j>0\\ j\neq\nu,\mu}}\mathcal{S}_j^2\\
&= \left(\sum_{\nu>0}\eta_\nu\eta_{\tilde{\nu}}\mathcal{S}_\nu\right)\left(\sum_{\mu>0}\mathcal{S}_\mu\eta_\mu\eta_{\tilde{\mu}}\right), \text{ since } \mathcal{S}_j^2 = \mathbf{1}.
\end{aligned}
\tag{A20}
$$

As

$$
\begin{aligned}
\eta_\nu\eta_{\tilde{\nu}}\mathcal{S}_\nu &= i\eta_\nu\eta_{\tilde{\nu}}\left(a_\nu + a_\nu^+\right)\left(a_{\tilde{\nu}} + a_{\tilde{\nu}}^+\right)\\
&= i\eta_\nu\left(a_\nu + a_\nu^+\right)\eta_{\tilde{\nu}}\left(a_{\tilde{\nu}} + a_{\tilde{\nu}}^+\right) = ia_\nu^+a_{\tilde{\nu}}^+
\end{aligned}
\tag{A21}
$$

and

$$
\mathcal{S}_\mu\eta_\mu\eta_{\tilde{\mu}} = \left(\eta_\mu\eta_{\tilde{\mu}}\mathcal{S}_\mu\right)^+ = -ia_{\tilde{\mu}}a_\mu, \tag{A22}
$$

we obtain

$$
R^2 = \sum_{\nu,\mu>0}a_\nu^+a_{\tilde{\nu}}^+a_{\tilde{\mu}}a_\mu = P^+P. \tag{A23}
$$

APPENDIX B: FLETCHER METHOD

To facilitate comparisons with our study, the Fletcher method [42] is recalled in this appendix.

A. Hamiltonian

We start with the Hamiltonian (1). To conserve the particle number on average, we define the auxiliary Hamiltonian as

$$
H = \mathcal{H} - \lambda N \tag{B1}
$$

where λ is the Fermi energy, and N is the particle number operator given by

$$
N = \sum_{\nu>0}\left(\eta_\nu + \eta_{\tilde{\nu}}\right). \tag{B2}
$$

The Hamiltonian H then reads as

$$
H = H_0 + H_1 \tag{B3}
$$

with the notations

$$
H_0 = \sum_{\nu>0}\tilde{\varepsilon}_\nu\left(\eta_\nu + \eta_{\tilde{\nu}}\right),\ H_1 = -GP^+P \text{ and } \tilde{\varepsilon}_\nu = \varepsilon_\nu - \lambda. \tag{B4}
$$

B. Grand partition function

The grand partition function can be written as

$$
\mathcal{Z} = \mathrm{Tr}\,\mathrm{e}^{-\beta H} \tag{B5}
$$

where β is the inverse of the system temperature T, and Tr is the trace over all the states of the system.

Using the same treatment as in Sec. II, we obtain

$$
\mathrm{e}^{-\beta H} = \mathrm{e}^{-\beta H_0}\mathsf{S}(\beta), \tag{B6}
$$

where

$$
\begin{aligned}
\mathsf{S}(\beta) &= \mathrm{e}^{\beta H_0}\mathrm{e}^{-\beta H}\\
&= T_\tau\exp\left(-\int_0^\beta H_1(\tau)\,\mathrm{d}\tau\right),
\end{aligned}
\tag{B7}
$$

T_τ is the chronological operator, and $H_1(\tau)$ is the Heisenberg transform of H_1.

$\mathsf{S}(\beta)$ may also be written as

$$
\mathsf{S}(\beta) = \lim_{N\to\infty}T_\tau\prod_{j=1}^{N}\exp\left[-\frac{\beta}{N}H_1\left(\tau_j\right)\right], \tag{B8}
$$

where $\tau_j = j\dfrac{\beta}{N},\ j = 1,2,...,N$.

To apply the Hubbard-Stratonovitch transformation (31), Fletcher assumes that $H_1\left(\tau_j\right)$ in Eq. (B8) may be expressed as

$$
H_1\left(\tau_j\right) = \theta_1\left(\tau_j\right)\theta_2\left(\tau_j\right) \tag{B9}
$$

with

$$
\theta_1 = \sqrt{G}P^+, \qquad \theta_2 = \sqrt{G}P. \tag{B10}
$$

Although θ_1 and θ_2 do not strictly commute because

$$
[\theta_1,\theta_2] = G\sum_\nu\left[a_\nu^+a_{\tilde{\nu}}^+, a_{\tilde{\nu}}a_\nu\right], \tag{B11}
$$

for small G (which is the case as it represents a residual interaction),

$$\exp\left[-\frac{\beta}{N}\theta_1\theta_2\right] = \exp\left[\left(\frac{1}{2}\sqrt{\frac{\beta}{N}}\frac{\theta_1-\theta_2}{2}\right)^2\right] \times \exp\left[\left(\frac{i}{2}\sqrt{\frac{\beta}{N}}\frac{\theta_1+\theta_2}{2}\right)^2\right] \quad \text{(B12)}$$

because

$$\theta_1\theta_2 = \left(\frac{\theta_1+\theta_2}{2}\right)^2 - \left(\frac{\theta_1-\theta_2}{2}\right)^2. \quad \text{(B13)}$$

By applying the Hubbard-Stratonovitch transformation to each exponential in Eq. (B12), we obtain

$$\exp\left[\left(\frac{1}{2}\sqrt{\frac{\beta}{N}}\frac{\theta_1-\theta_2}{2}\right)^2\right] = \int_{-\infty}^{+\infty} \mathrm{d}x_j \exp\left\{-\pi x_j^2 - \sqrt{\frac{\pi\beta}{N}}(\theta_1-\theta_2)x_j\right\} \quad \text{(B14)}$$

and

$$\exp\left[\left(\frac{i}{2}\sqrt{\frac{\beta}{N}}\frac{\theta_1+\theta_2}{2}\right)^2\right] = \int_{-\infty}^{+\infty} \mathrm{d}y_j \exp\left\{-\pi y_j^2 - i\sqrt{\frac{\pi\beta}{N}}(\theta_1+\theta_2)y_j\right\} \quad \text{(B15)}$$

with the notations

$$x_j = x(\tau_j) \text{ and } y_j = y(\tau_j). \quad \text{(B16)}$$

Using the change of variables

$$x_j = \sqrt{\frac{\beta}{N}}X_j \text{ and } y_j = \sqrt{\frac{\beta}{N}}Y_j, \quad \text{(B17)}$$

Eq. (B12) takes the form

$$\exp\left[-\frac{\beta}{N}\theta_1\theta_2\right] = \lim_{N\to\infty}\prod_{j=1}^{N}\frac{\beta}{N}\int_{-\infty}^{+\infty}\mathrm{d}X_j\int_{-\infty}^{+\infty}\mathrm{d}Y_j \exp\left\{-\frac{\pi\beta}{N}\left(X_j^2+Y_j^2\right) - \sqrt{\pi}\frac{\beta}{N}\left[\left(X_j+iY_j\right)\theta_1(\tau_j) - \left(X_j-iY_j\right)\theta_2(\tau_j)\right]\right\}. \quad \text{(B18)}$$

Let us introduce the notations

$$\int \mathfrak{D}X = \lim_{N\to\infty}\int_{-\infty}^{+\infty}\prod_{j=1}^{N}\sqrt{\frac{\beta}{N}}\mathrm{d}X_j \quad \text{(B19)}$$

and

$$\int \mathfrak{D}Y = \lim_{N\to\infty}\int_{-\infty}^{+\infty}\prod_{j=1}^{N}\sqrt{\frac{\beta}{N}}\mathrm{d}Y_j. \quad \text{(B20)}$$

It is worth noting that when the limit is taken, $X_j \to X(\tau)$ and $Y_j \to Y(\tau)$.

We also define the complex function

$$z(\tau_j) = X_j(\tau_j) + iY_j(\tau_j) = X_j + iY_j. \quad \text{(B21)}$$

As

$$\frac{1}{2}\int \mathfrak{D}z\mathfrak{D}\bar{z} = \int \mathfrak{D}X\mathfrak{D}Y, \quad \text{(B22)}$$

and

$$\int_0^\beta f(X(\tau))\mathrm{d}\tau = \lim_{N\to\infty}\frac{\beta}{N}\sum_{j=1}^{N} f\left(X(\tau_j)\right) = \lim_{N\to\infty}\frac{\beta}{N}\sum_{j=1}^{N} f\left(X_j\right), \quad \text{(B23)}$$

where $f(x)$ is any integrable function on the interval $[0,\beta]$, we obtain

$$\mathsf{S}(\beta) = \frac{1}{2}\int \mathfrak{D}z\mathfrak{D}\bar{z}\exp\left[-\pi\int_0^\beta |z(\tau)^2|\mathrm{d}\tau\right] \times T_\tau \exp\left\{\sqrt{\pi}\int_0^\beta [z(\tau)\theta_1(\tau) - \bar{z}(\tau)\theta_2(\tau)]\mathrm{d}\tau\right\}. \quad \text{(B24)}$$

Finally, when replacing $\theta_1(\tau)$ and $\theta_2(\tau)$ with their respective expressions, and using Eq. (B6), the partition function becomes

$$\mathcal{Z} = \mathrm{Tr}\left\{\mathrm{e}^{-\beta H_0}\frac{1}{2}\int \mathfrak{D}z\mathfrak{D}\bar{z}\exp\left[-\pi\int_0^\beta |z(\tau)^2|\mathrm{d}\tau\right] \times T_\tau \exp\left[-\int_0^\beta H'(\tau)\mathrm{d}\tau\right]\right\}, \quad \text{(B25)}$$

where we set

$$H'(\tau) = \sqrt{\pi G}\sum_{\nu>0}\left[a_\nu^+(\tau)a_{\tilde{\nu}}^+(\tau)z(\tau) + \bar{z}(\tau)a_{\tilde{\nu}}(\tau)a_\nu(\tau)\right]. \quad \text{(B26)}$$

In the case of the static path approximation, it is assumed that $X(\tau)$ and $Y(\tau)$, and thus $z(\tau)$, are independent from

the imaginary time τ. The functional integral in Eq. (B25) then reduces to an ordinary integral and is given by

$$\mathcal{Z} = \frac{1}{2}\int \mathrm{d}z\mathrm{d}\bar{z}\exp\left[-\pi\int_0^\beta |z|^2\mathrm{d}\tau\right]\mathrm{Tr}\mathrm{e}^{-\beta H'}, \tag{B27}$$

where

$$H' = \sum_{\nu>0}\left[\tilde{\varepsilon}_\nu(\eta_\nu+\eta_{\bar{\nu}}) - \sqrt{\pi G}\left(z a_\nu^+ a_{\bar{\nu}}^+ + \bar{z}a_{\bar{\nu}}a_\nu\right)\right]. \tag{B28}$$

The trace of $\mathrm{e}^{-\beta H'}$ may be easily evaluated in its eigenbasis. Moreover, H' may be written in the matrix form

$$H' = \sum_{\nu>0} V_\nu^+ A_\nu V_\nu + \sum_{\nu>0}\tilde{\varepsilon}_\nu \tag{B29}$$

where we set

$$V_\nu^+ = \left(a_\nu^+, -a_{\bar{\nu}}\right),\ A_\nu = \begin{pmatrix} \tilde{\varepsilon}_\nu & \Delta \\ \Delta & -\tilde{\varepsilon}_\nu \end{pmatrix} \text{ and } \Delta = \sqrt{\pi G}z. \tag{B30}$$

The quantity Δ is interpreted as the gap parameter. Hereafter, it is assumed to be real.

The matrix A_ν is diagonalized such that

$$A_\nu = T_\nu^+ D_\nu T_\nu \tag{B31}$$

where

$$T_\nu = \begin{pmatrix} u_\nu & v_\nu \\ v_\nu & -u_\nu \end{pmatrix},\ D_\nu = \begin{pmatrix} E_\nu & 0 \\ 0 & -E_\nu \end{pmatrix} \tag{B32}$$

with

$$E_\nu = \sqrt{\tilde{\varepsilon}_\nu^2+\Delta^2} \text{ and } \left.\begin{matrix} u_\nu^2 \\ v_\nu^2 \end{matrix}\right\} = \frac{1}{2}\left(1\pm\frac{\tilde{\varepsilon}_\nu^2}{E_\nu}\right). \tag{B33}$$

The Hamiltonian H' then takes the diagonal form

$$H' = \sum_{\nu>0} W_\nu^+ D_\nu W_\nu + \sum_{\nu>0}\tilde{\varepsilon}_\nu \tag{B34}$$

where

$$W_\nu = T_\nu V_\nu. \tag{B35}$$

It is now possible to calculate the trace in Eq. (B27), which becomes

$$\mathcal{Z} = \frac{1}{2}\int \mathrm{d}z\mathrm{d}\bar{z}\mathrm{e}^{-\beta F}, \tag{B36}$$

where the free energy F is given by

$$F = \sum_{\nu>0}\left[\tilde{\varepsilon}_\nu - \frac{1}{\beta}\ln\left(4\cosh^2\frac{\beta}{2}E_\nu\right)\right] + \frac{\Delta^2}{G}. \tag{B37}$$

C. Gap Equations - Statistical quantities

The saddle-point approximation reads as

$$\frac{\partial F}{\partial\Delta} = 0. \tag{B38}$$

Indeed, the dominant contribution to the partition function is found by determining the minimum value of the exponent in Eq. (B36). We then obtain

$$\frac{2}{G} = \sum_\nu \frac{1}{E_\nu}\tanh\left(\frac{\beta}{2}E_\nu\right). \tag{B39}$$

The latter equation is the typical FTBCS expression [7, 9, 46, 48]. The path integral method thus enables us to retrieve the standard FTBCS results by applying a saddle-point approximation.

The grand potential Ω is given by

$$\Omega = -\beta F \tag{B40}$$

and the particle-number is defined by Eq. (53).

We then have

$$N = \sum_\nu\left[1 - \frac{\tilde{\varepsilon}_\nu}{E_\nu}\tanh\left(\frac{\beta}{2}E_\nu\right)\right]. \tag{B41}$$

The energy of the system is defined by Eq. (57). Thus,

$$E = \sum_\nu \varepsilon_\nu\left[1 - \frac{\tilde{\varepsilon}_\nu}{E_\nu}\tanh\left(\frac{\beta}{2}E_\nu\right)\right] - \frac{\Delta^2}{G}. \tag{B42}$$

As for the entropy, using definition (59), we have

$$S = -\beta\sum_\nu E_\nu\tanh\left(\frac{\beta}{2}E_\nu\right) + \sum_\nu \ln\left(4\cosh^2\left(\frac{\beta}{2}E_\nu\right)\right). \tag{B43}$$

Finally, the heat capacity of the system defined by

$$C = -\beta\frac{\partial S}{\partial\beta} \tag{B44}$$

reads as

$$C=\frac{1}{2}\sum_{\nu}\left(\beta^2E_\nu^2+\beta^3\Delta\frac{\partial\Delta}{\partial\beta}\right)\frac{1}{\cosh^2\left(\frac{\beta}{2}E_\nu\right)}, \tag{B45}$$

with

$$\frac{\partial\Delta}{\partial\beta}\left[\sum_{\nu}\frac{\Delta}{E_\nu}\tanh\frac{\beta}{2}E_\nu-\frac{\beta}{2}\sum_{\nu}\frac{\Delta}{E_\nu^2}\frac{1}{\cosh^2\frac{\beta}{2}E_\nu}\right]=\frac{1}{2}\sum_{\nu}\frac{1}{\cosh^2\left(\frac{\beta}{2}E_\nu\right)}. \tag{B46}$$

References

[1] A. Bohr, B. R. Mottelson, and D. Pines, Phys. Rev. **110**(4), 936 (1958)
[2] J. Bardeen, L. N. Cooper, and J. R. Schrieffer, Phys. Rev. **108**(5), 1175 (1957)
[3] S. T. Belyaev, Mat. Fys. Medd. Dan. Vid. Selsk. **31**, 11 (1959)
[4] A. Ravlic, E. Yuksel, T. Niksic *et al.*, Nat. Commun. **14**, 4834 (2023)
[5] A. Kaur, E. Yuksel and N. Paar, Phys. Rev. C **109**, 014314 (2024)
[6] A. Kaur, E. Yuksel, and N. Paar, Phys. Rev. C **109**, 044305 (2024)
[7] M. Sano and S. Yamazaki, Prog. Theor. Phys. **29**(3), 397 (1963)
[8] L. G. Moretto, Nucl. Phys. A **185**(1), 145 (1972)
[9] A.L. Goodman, Phys. Rev. C **29**(5), 1887 (1984)
[10] H. Nakada and K. Tanabe, Int. J. Mod. Phys. E **15**(8), 1761 (2006)
[11] Z. Kargar, Phys. Rev. C **75**, 064319 (2007)
[12] N. H. Allal, M. Fellah, N. Benhamouda *et al.*, Phys. Rev. C **77**, 054310 (2008)
[13] D. Gambacurta, D. Lacroix, and N. Sandulescu, Phys. Rev. C **88**, 034324 (2013)
[14] A. Goodman, Nucl. Phys. A **352**(1), 30 (1981)
[15] K. Tanabe, K. Sugawara-Tanabe, and H.J. Mang, Nucl. Phys. A **357**(1), 20 (1981)
[16] L. Liu, Z.-H. Zhang, and P.-W. Zhao, Phys. Rev. C **92**, 044304 (2015)
[17] P. Fanto, Y. Alhassid, and G. F. Bertsch, Phys. Rev. C **96**, 014305 (2017)
[18] E. Yüksel, F. Mercier, J.-P. Ebran *et al.*, Phys. Rev. C **106**, 054309 (2022)
[19] O. Civitarese, G. G. Dussel, and R.P.J. Perazzo, Nucl. Phys. A **404**(1), 15 (1983)
[20] A. Storozhenko, P. Schuck, J. Dukelsky *et al.*, Annals of Physics **307**(2), 308 (2003)
[21] N. Dinh Dang and N. Quang Hung, Phys. Rev. C **77**, 064315 (2008)
[22] P. Fanto and Y. Alhassid, Phys. Rev. C **103**, 064310 (2021)
[23] D. J. Dean and M. Hjorth-Jensen, Rev. Mod. Phys. **75**(2), 607 (2003)
[24] A. Ravlić, Y. F. Niu, T. Nikšić, N. Paar *et al.*, Phys. Rev. C **104**, 064302 (2021)
[25] W. Zhang and Y.-F. Niu, Chin. Phys. C **41**, 094102 (2017)
[26] T. Yan, Y. L. Lin, and L. Liu, Phys. Rev. C **104**, 024303 (2021)
[27] W. Zhang, J.-K. Huang, and Yi-Fei Niu, Int. J. Mod. Phys. E **32**, 2340008 (2023)
[28] Y. H. Gao, Y. L. Lin, and L. Liu, Int. J. Mod. Phys. E **32**, 2350050 (2023)
[29] A. Ravlić, E. Yüksel, T. Nikšić *et al.*, arXiv: 2309.09302v1
[30] E. Litvinova and P. Schuck, Phys. Rev. C **104**, 044330 (2021)
[31] M. Drissi and A. Rios, Eur. Phys. J. A **58**, 90 (2022)
[32] K. Langanke, P. Vogel, and D.-C. Zhen, Nucl. Phys. A **626**(3), 735 (1997)
[33] S. E. Koonin, D. J. Dean, and K. Langanke, Phys. Rep. **278**(1), 1 (1997)
[34] Y. Alhassid, G. F. Bertsch, C. N. Gilbreth *et al.*, Phys. Rev. C **93**, 044320 (2016)
[35] G. Puddu, Phys. Rev. B **45**(17), 9882 (1992)
[36] G. Puddu, Phys. Rev. C **47**(3), 1067 (1993)
[37] M. Marinus, H. G. Miller, R. M. Quick *et al.*, Phys. Rev. C **48**(4), 1713 (1993)
[38] R. Rossignoli, N. Canosa, and J. L. Egido, Nucl. Phys. A **605**(1), 1 (1996)
[39] N. Canosa and R. Rossignoli, Phys. Rev. C **56**(2), 791 (1997)
[40] N. Canosa, R. Rossignoli, and P. Ring, Phys. Rev. C **59**(1), 185 (1999)
[41] K. Kaneko and A. Schiller, Phys. Rev. C **76**, 064306 (2007)
[42] G. Fletcher, Am. J. Phys. **58**, 50 (1990)
[43] J. Hubbard, Phys. Rev. Lett. **3**(2), 77 (1959)
[44] R. L. Stratonovich, Sov. Phys. Dokl. **2**, 416 (1958)
[45] M. Fellah, N. H. Allal, M. Belabbas *et al.*, Phys. Rev. C **76**, 047306 (2007)
[46] M. Belabbas, M. Fellah, N. H. Allal, *et al.*, Int. J. Mod. Phys. E **19**(10), 1973 (2010)
[47] I. Ami, M. Fellah, N. H. Allal *et al.*, Int. J. Mod. Phys. E **20**(9), 1947 (2011)
[48] D. Mokhtari, N. H. Allal, and M. Fellah, Int. J. Mod. Phys. E **27**, 1850054 (2018)
[49] Y. Alhassid and J. Zingman, Phys. Rev. C **30**(2), 684 (1984)
[50] P. Ring and P. Schuck, *The Nuclear Many Body Problem*, (Springer, Berlin, 1980).
[51] D. Gambacurta and D. Lacroix, Phys. Rev. C **85**, 044321 (2012)
[52] T. Sumaryada and A. Volya, Phys. Rev. C **76**, 024319 (2007)
[53] N. H. Allal and M. Fellah, Phys. Rev. C **50**(3), 1404 (1994)
[54] F. Simkovic, Ch. C. Moustakidis, L. Pacearescu and A. Faessler, Phys. Rev. C **68**, 054319 (2003)
[55] E. Melby *et al.*, Phys. Rev. Lett. **83**(16), 3150 (1999)
[56] A. Schiller, A. Bjerve, M. Guttormsen *et al.*, Phys. Rev. C **63**, 021306 (2001)
[57] K. Esashika, H. Nakada, and K. Tanabe, Phys. Rev. C **72**, 044303 (2005)